

NANOCRYSTALLINE INCOMMENSURATE STRUCTURES IN Ti-TM ALLOYS

Nataliya B. Dyakonova, Igor V. Lyasotsky and Galina I. Nosova

I.P.Bardin Central research institute for iron and steel industry, 2-nd Baumanskaya 9/23, 105005 Moscow, Russia

Received: March 29, 2008

Abstract. Nanocrystalline ω structures in quenched $Ti_{1-x}V_x$ ($x=0.13-0.40$) and $Ti_{1-y}Fe_y$ ($y=0.065-0.20$) were studied by means of XRD and TEM methods. XRD data at 20 °C and -195 °C were obtained for monocrystalline samples. Anomalous reversible increase of peak intensities of ω reflections at low temperature accompanied by decrease of their width was observed for alloys with valence electron concentrations 4.19-4.25 e/a. Correlation between temperature dependences of intensity of ω reflections and resistivity was observed for alloys in the quenched state and after low temperature annealing. The nature of nanoscale structures consisting of ω clusters of 4 different crystallographic orientations in BCC matrix is discussed in connection with electronic structure of the alloys.

1. INTRODUCTION

Nanocrystalline structures in metal alloys are usually formed by diffusion controlled processes of decomposition into different phases. However nanoscale phase separation by diffusionless mechanism of atomic shuffles is also possible.

Omega phase and related incommensurate structure ("diffuse" ω -phase) in Ti base alloys is an example of a spontaneously formed nanocrystalline structure [1,2] with specific properties, in particular anomalous temperature dependence of resistivity [3,4]. Hexagonal (or rhombohedral) ω -phase is formed in alloys of Ti with 3d and 4d elements with electron concentrations $C_e \sim 4.1-4.2$ electron to atom quenched from high temperature body centered cubic β -phase. It always precipitates as nanosize particles in the BCC β -phase matrix with orientation $[00.1]\omega // \langle 111 \rangle \beta$. Structure of ω -phase can be represented as commensurate modulation with period $3d_{111}$ along $\langle 111 \rangle$ direction of the parent BCC β -phase. The transformation of β -phase into so called athermal ω -phase can be accomplished solely by shuffles of atoms at short dis-

tances, so no diffusion is necessary. The particles of the 4 possible orientations corresponding to four $\langle 111 \rangle$ directions of a cubic lattice form a nanocrystalline structure with low volume fraction of the residual β -phase (however, it is difficult to evaluate the exact volume fraction due to coincidence of reflections from β -phase with those from ω -phase) [1,2,5,6]. Volume fractions of the 4 orientations are equal if no stress or deformation is applied.

Incommensurate structures on the base of BCC phase ("diffuse" ω -phase) are observed in titanium alloys with higher C_e . Practically all the presented structure models consistent with TEM and XRD experiments are one-dimensional, i.e. modulation of the parent BCC lattice occurs along only one of the four possible $\langle 111 \rangle$ directions [2,7]. However diffuse ω -phase also exists in the form of nanocrystalline mixture of particles of the 4 orientations.

The aim of this work was characterization of the nanocrystalline structure in Ti-V and Ti-Fe alloys and its evolution with alloy composition and

Corresponding author: N.B.Dyakonova, e-mail: n-dyakonova@yandex.ru

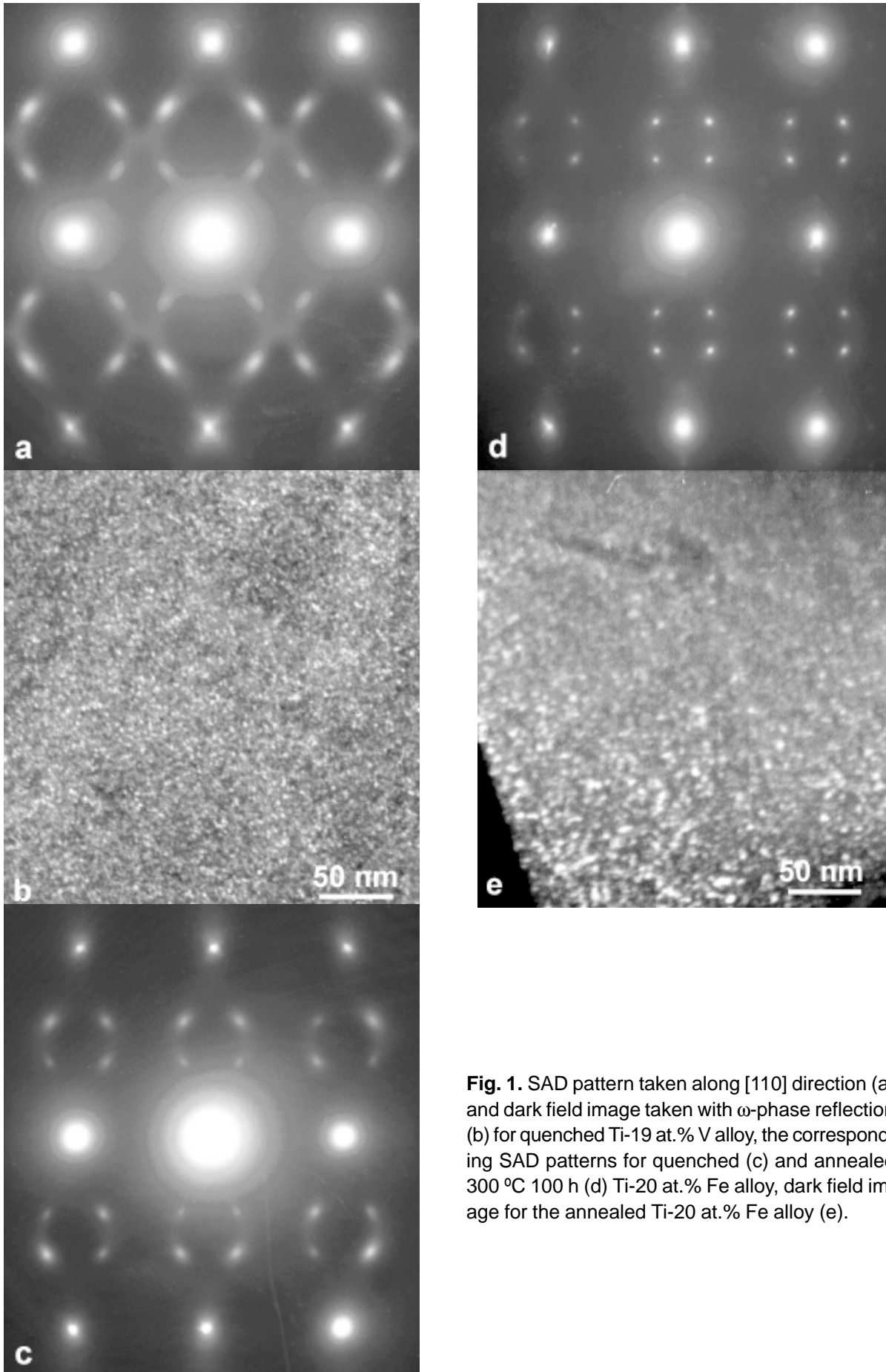


Fig. 1. SAD pattern taken along $[110]$ direction (a) and dark field image taken with ω -phase reflection (b) for quenched Ti-19 at.% V alloy, the corresponding SAD patterns for quenched (c) and annealed 300 °C 100 h (d) Ti-20 at.% Fe alloy, dark field image for the annealed Ti-20 at.% Fe alloy (e).

temperature. The impact of low temperature heat treatment upon structure and electrical conductivity has also been studied.

2. EXPERIMENT

The alloys were prepared by arc melting of pure Ti, V and Fe in argon atmosphere. The ingots were annealed at 900 – 1200 °C and then quenched in iced brine. Large grains grown during the anneal were cut from the ingots and used as monocrystalline samples for X-ray diffraction (XRD) study. The intensity measurements were carried out using Mo K_{α} radiation and results were corrected for absorption, polarization and geometrical factors. Samples for TEM and resistivity measurements were cut from the same pieces of the ingots as the samples for XRD study.

3. RESULTS

Titanium base alloys with V (13, 17, 19, 23, 28 and 40 at.%) and Fe (5.5, 6, 9.5, 12.5, 14.5 and 20 at.%) have been investigated by TEM and XRD methods. Fig. 1 shows an example of SAD pattern and dark field TEM image (taken with ω -reflection which does not overlap with any BCC reflection and corresponds to one of the 4 possible orientations) for quenched Ti-19%V alloy. For this composition ω -reflections are only slightly shifted from their positions and they are more diffuse than for alloys with lower V content in agreement with the previous results [1].

3.1. Dependence on composition

Nanocrystalline structure with w particle size 6 – 8 nm is observed for quenched Ti-V alloys in the composition range 13 – 17 at.% V. In transition composition range (~19% to 40%) ω reflections in TEM and XRD diffraction patterns shift from their positions characteristic for the ω -phase ($2/3\ 2/3\ 2/3$ and equivalent positions in reciprocal lattice of the BCC β -phase) along $\langle 111 \rangle$ away from the nearest reflection of the BCC lattice, i.e. structure changes from commensurate to incommensurate. Simultaneously the width of diffraction maxima increases both in $\langle 111 \rangle$ and in perpendicular, e.g. $\langle 211 \rangle$, reciprocal lattice directions.

The ω particle size was estimated from the width of ω -like reflections using the expression $D = \lambda / (B_h \cos \theta)$, where λ is the wavelength of the radiation used, 2θ – the scattering angle, B_h – half maximum full width (HMFV) corrected for instrumental broadening. The form of reflections was fitted (by

least squares method, after phase subtraction) by the function of the form $f(x) = A / (1 + (x - C)^2 / B^2)^2$.

Particle size decreases rather sharply to ~1 - 2 nm with increasing concentration of vanadium in Ti-V system (Fig. 2). Qualitatively the same dependence holds for quenched Ti-Fe alloys for compositions within similar range of electron concentrations (C_e) (Fig. 2b). At higher Fe concentrations (~20 at.%) mean particle size increases again as the diffuse reflections approach another commensurate position $4/5\ 4/5\ 4/5$ (indexes of the BCC phase reciprocal lattice). Example of SAD pattern for this case is shown in Fig. 1c.

3.2. Dependence on temperature

Reversible variations of intensity of diffuse ω -reflections are observed in the temperature range -195 - +20 °C for both Ti-V and Ti-Fe quenched alloys (Fig. 3). The most prominent effects are observed in transition composition range around electron concentration $C_e \sim 4.2$ el./atom for Ti-V alloys. Increase of intensity by cooling is much larger than that expected from decrease of Debay-Waller factor at low temperatures. For example, for one of the most strong ω reflections located near the position $4/3\ 4/3\ 4/3$ of β -phase reciprocal lattice the increase of intensity by cooling from 20 to -195 °C at the expense of Debay-Waller factor could constitute only ~10% (if we suppose Debay temperature to take a rather low value of 200K), while experimental ratios of intensities are 4 -5 times for alloys with 19 - 23% V (Figs. 3a and 4). For Ti-Fe system maximum value of intensity ratio is much lower: ~1.4 (e.g. Fig. 3b). With increasing content of the alloying element intensity ratio becomes smaller approaching 1 (Debay-Waller factor for ω -reflections is lower than for fundamental reflections of the BCC phase due to larger width, so that the measured intensity includes contribution from thermal scattering). Difference in width of ω reflections (and hence particle size) also approaches zero as V or Fe content increases beyond the transition interval (Fig. 2).

Intensity ratio of diffraction maxima for the two temperatures versus composition (Fig. 4) is shown for $4/3\ 4/3\ 4/3$ reflection, but the ratios for other reflections are close to these values, i.e. relative intensities of different reflections do not change significantly. As the structure factor of reflections depends on atomic displacements from BCC lattice sites it can be concluded that the displacements of atoms in ω -configurations only slightly increase when the temperature is lowered. Relative inten-

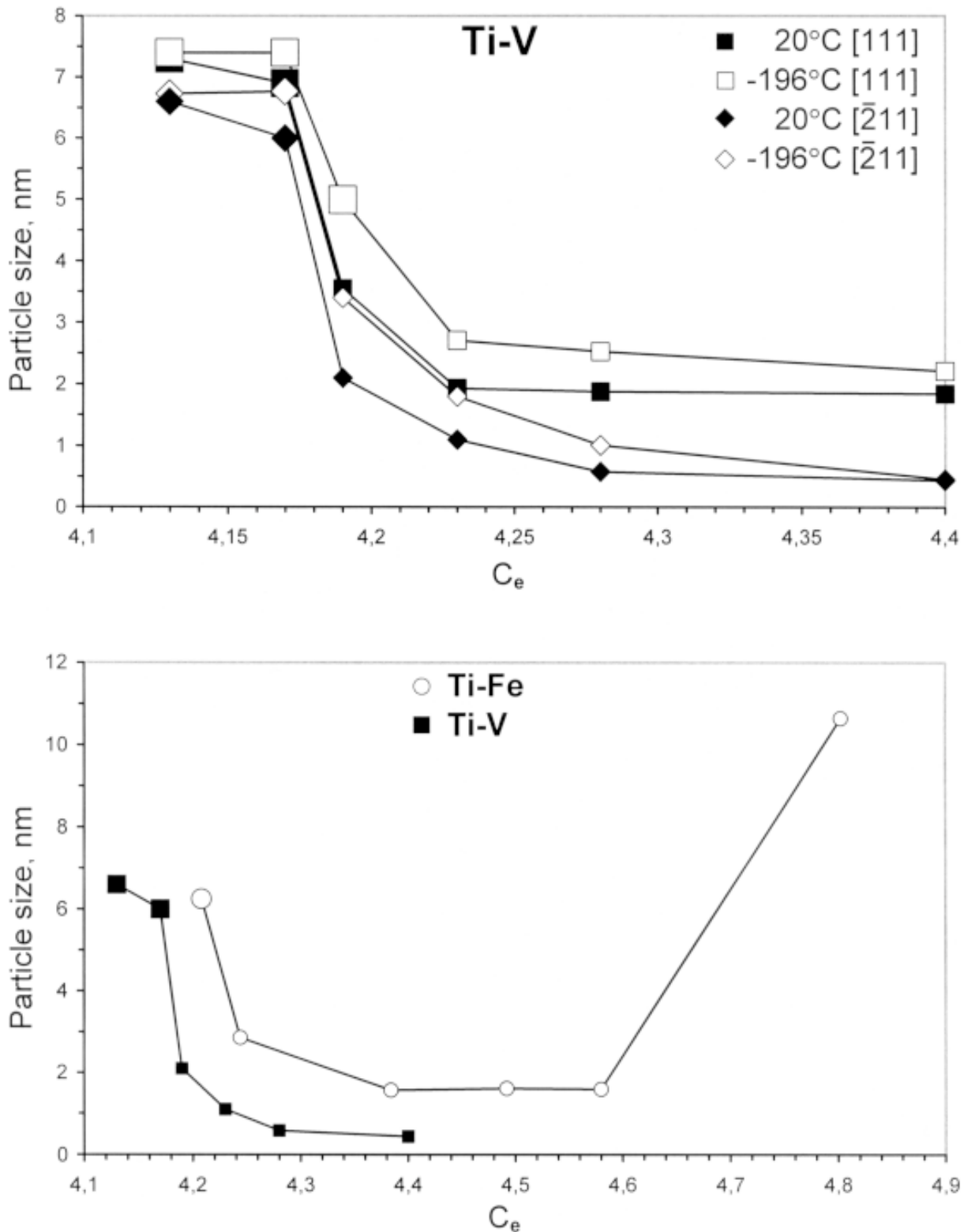


Fig. 2. Dependence of particle size (calculated from width of XRD peaks) on electron concentration for Ti-V alloys (a) and Ti-Fe (b). Values of particle size in [111] and perpendicular $\langle 211 \rangle$ directions for two temperatures (+20° and -195 °C) are shown for Ti-V alloys (a). Alongside with particle size in perpendicular $\langle 211 \rangle$ directions at +20 °C for Ti-Fe alloys Fig.1b shows the corresponding curve for Ti-V alloys for comparison. Size of the squares designating experimental points along the y-axis corresponds to the estimated error.

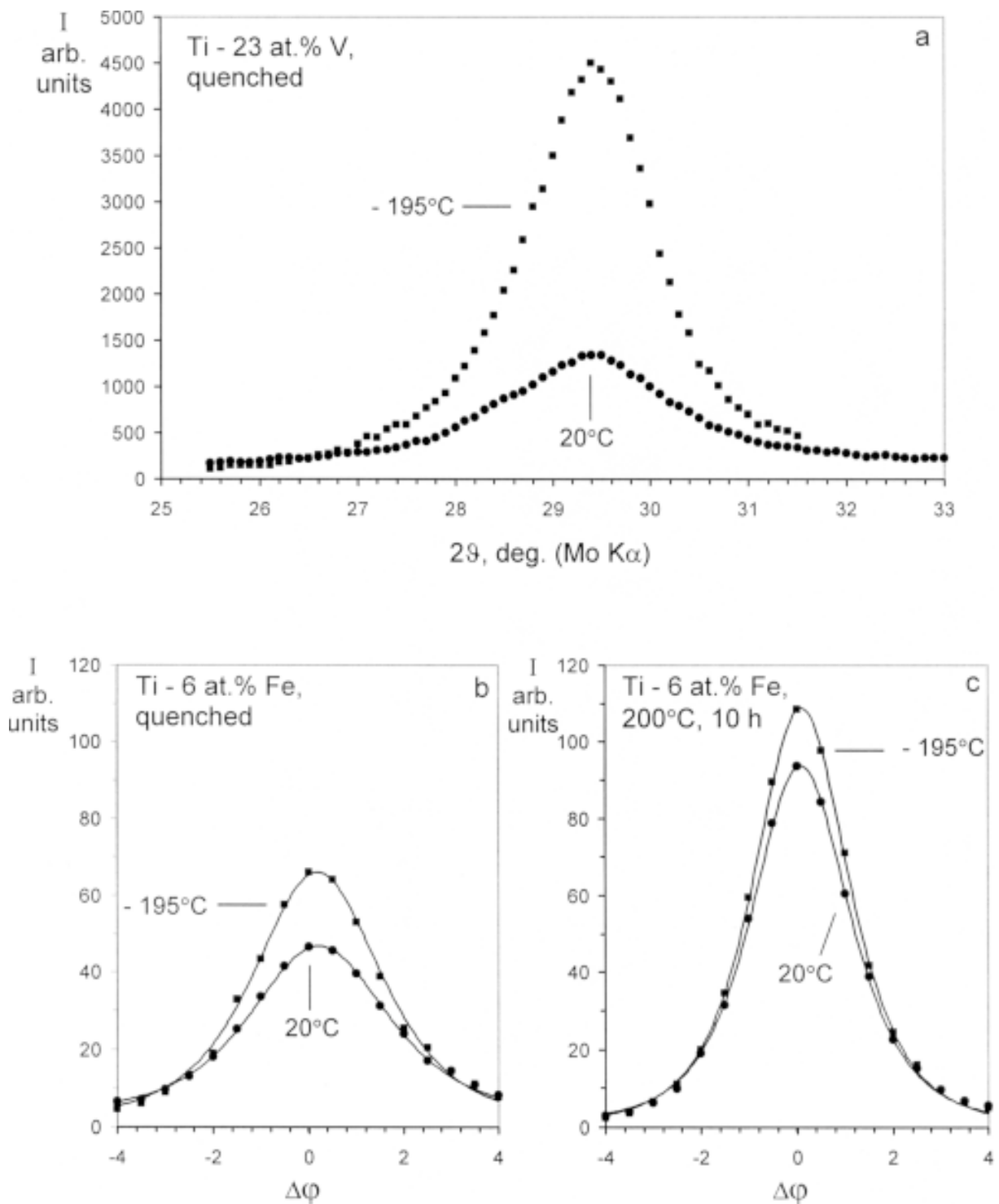


Fig. 3. Experimental XRD scans through ω -like diffuse maximum near $(h k l)_{\text{BCC}} = 4/3 \ 4/3 \ 4/3$ for Ti-23 at.% V (scan along $[111]$) and for quenched and annealed Ti-6 at.% Fe alloys (scan along $\langle 211 \rangle$) taken at two temperatures ($+20^\circ$ and -195°C).

sities can be calculated for a model structure constructed of ω -like atomic configurations. The value of atomic displacements (Δ) can be estimated by

fitting the calculated intensities to experiment. For Ti-V alloys Δ decreases sharply from $0.5d_{111}$ to $0.25d_{111}$ in the same transition concentration range.

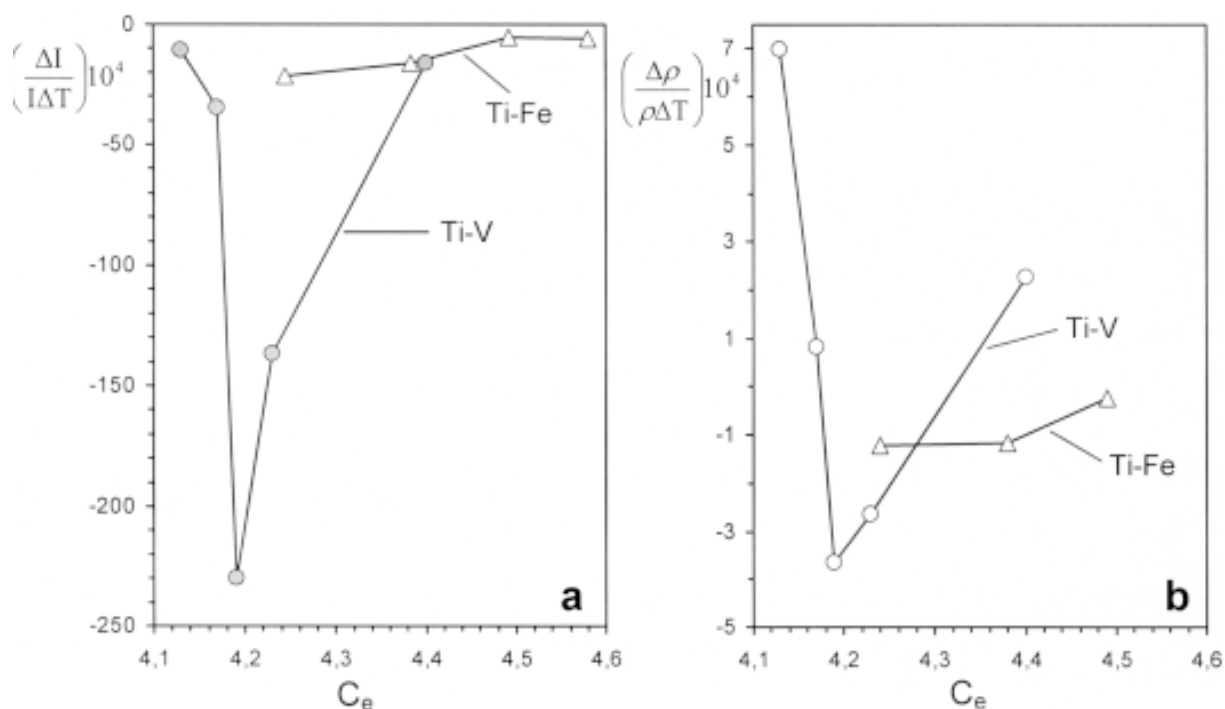


Fig. 4. Correlation between temperature dependences of the peak intensity of diffuse ω reflections and resistivity. Temperature coefficient of the intensity ($TCI = \Delta I / I \Delta T$) for reflection near $(hkl)_{\text{BCC}} = (4/3 \ 4/3 \ 4/3)$ (a) and temperature coefficient of resistivity ($TCR = \Delta \rho / \rho \Delta T$) (b) versus electron concentration for Ti-V and Ti-Fe quenched alloys.

The largest growth of Δ by cooling to -195°C is observed for Ti-23%V alloy.

Maximum intensity ratio also corresponds to transition composition range and constitutes as much as 5 times for Ti-19 at.% V alloy. However the ratio of the corresponding integral intensities for the same reflections is much lower, as the width of reflections decreases when the temperature is lowered. Integral intensities were estimated as $I_{\text{int}} \sim I_m * B_{111} * B_{211}^2$, where B_{111} and B_{211} are half maximum full width in $\langle 111 \rangle$ direction parallel to the wave vector of displacement modulation and in $\langle 211 \rangle$ perpendicular directions, I_m – maximum intensity. The largest growth of integral intensity of the most strong w reflection near $4/3 \ 4/3 \ 4/3$ position is observed for Ti-23%V alloy, however it does not exceed 30%. For estimation of the change of volume fractions this value should be corrected for the variation of structure factor due to the increase of atomic shuffles in ω configurations from 0.025 to 0.031 d_{111} (deduced from the observed relative intensities of different ω reflections [6]). If such a

correction is made, volume fraction of w -particles does not change at all (though the error of this estimate is rather large $\sim \pm 10\%$).

3.3. Low temperature annealing

Structure changes caused by low temperature annealing of alloys with incommensurate ω -phase resemble those by cooling if the temperature is kept low enough to prevent diffusion controlled reaction of precipitation of Ti-rich ω and α phases. For most alloys reflections from the “diffuse” ω phase remain in the incommensurate positions, they become stronger but sharper (as shown in Figs. 1c and 1d for Ti-20%Fe alloy), so that integral intensity change is small. For alloys in transition composition range reflections from annealed samples also increase when the temperature is lowered, but the relative difference becomes smaller than for quenched samples (Figs. 3b and 3c, Table 1).

Thus low temperature heat treatments (at 200 – 300 $^\circ\text{C}$ depending on composition) lead to coars-

Table 1. Composition, heat treatment, temperature coefficients of intensity for diffuse w reflection nearest to (4/3 4/3 4/3) vertex and temperature coefficient of resistivity in the temperature range from -195 to +20 °C, relative difference between resistivity of samples annealed at 200 °C and quenched samples, displacement of XRD reflections from vertices of ω -phase reciprocal lattice, average ω -particle size (in $\langle 211 \rangle$ direction).

composition at.%	heat treatment	$\Delta I / \Delta T,$ $10^{-4}K^{-1}$	$\Delta \rho / \rho \Delta T,$ $10^{-4}K^{-1}$	$(\rho_a - \rho_q) / \rho_q$	$d,$ S_{222}	particle size, nm
Ti-6Fe	Quenched	-22	-1.25	-0.017	0.011	2.6
	200 °C 10 h	-8	+1.01	-0.017	0.011	3.3
Ti-9.5Fe	Quenched	-16	-1.16	+0.006	0.027	1.5
	200 °C 10 h	-10	-0.27	+0.006	0.026	1.7
Ti-12.5Fe	Quenched	-5	-0.23	-0.004	0.033	1.5
	200 °C 10 h	-6	+0.10	-0.004	0.034	1.5
Ti-23V	Quenched	-133	-2.62	-	0.012	1.9
	200 °C 10 h	-24	-1.71	-	0.007	3.4

ening of nanostructure, though particle size still remains in nanoscale interval (Table 1, Fig. 1e), while the volume fraction remains approximately the same. At the same time variations with temperature become smaller, i.e. structure stabilization occurs probably due to redistribution of different atomic species fitted to atomic displacements during heat treatment.

3.4. Resistivity.

Alloys of Ti with 3d elements are known to exhibit anomalous temperature dependences of resistivity below the ambient temperature in composition ranges adjacent to those corresponding to formation of athermal ω -phase [3, 4]. In particular $\rho(T)$ dependences are nearly linear functions on temperature with negative temperature coefficients of resistivity (TCR) in the interval -195 - + 100 °C.

For the quenched Ti-23%V and Ti-6.5-12.5%Fe alloys TCR is negative while after annealing TCR either becomes positive or remains negative but with the lower absolute value. TCR correlates with temperature dependence of intensities of ω reflections (Fig. 4). The larger is increase of intensity by cooling the higher is the absolute value of negative TCR for both systems though the dependences are quantitatively different for Ti-V and Ti-Fe alloys. For the investigated alloys TCR is negative only for those alloys for which anomalously large increase of intensity of ω -like reflections (and particle growth) is observed by cooling.

4. DISCUSSION

Large reversible increase of the peak intensities of ω reflections observed by cooling the investigated alloys with $C_e \sim 4.19-4.24$ are accompanied by decrease of their width, so that variations of integral intensities which are proportional to the volume fraction of ω -clusters are much smaller. This result is in agreement with the estimate of volume fraction ($\sim 50\%$) for Zr-20 at.%Nb alloy [8] for which C_e and diffraction patterns are almost similar to those for Ti-19%V alloy. According to [8] ω peak intensity increases by ~ 1.6 times while the volume fraction changes are less than 2% when the alloy is cooled to -195 °C. For the investigated Ti based alloys the volume fraction of ω particles or ω -like configurations in the incommensurate ω -phase (more than 50% [6]) only slightly increases or does not change at all when the alloys are cooled to -195 °C. Simultaneously the average particle size grows up to 1.5 – 1.7 times for these alloys, however nanoscale ($\sim 2-7$ nm) structure is maintained.

According to the obtained results the particle size of nanocrystalline structure reversibly changes with temperature, gradual structure changes are realized via diffusionless mechanism of atomic shuffles, so that at each temperature the alloy is in a metastable state.

Formation of the observed metastable incommensurate structure is dominated by electron structure of the alloys [2,5]. This conclusion is supported by dependence of position of diffuse maxima on

electron concentration of the alloys but not on their atomic compositions as was pointed out in [2,5]. Increase of resistivity with enhancement of order (increasing particle size with lowering temperature or by low temperature annealing) observed in this work is also a characteristic feature for such interactions. Correlation between variations of intensity of reflections and resistivity is also in favor of this conclusion.

Anomalies of conductivity (high resistivity, negative temperature coefficient of resistivity) for Ti-V and Ti-Fe alloys can be adequately described by diffraction model [9,10]. Resistance increases when intensity of diffraction maxima observed by XRD increase with lowering temperature or with low temperature annealing. In the transition composition range anomalous increase of diffraction maxima occurs by cooling mainly due to particle growth. It is much larger than possible intensity increase due to temperature dependence of Debay-Waller factor. Negative temperature coefficients of resistivity are observed only in case of the anomalously large reversible variations of diffraction maxima with temperature.

The origin of incommensurate structure modulation accompanied by anomalies of conductivity is assumed to be connected to specific topology of Fermi surface. However in the case considered symmetry is such that the decrease of enthalpy can not be achieved by superposition of the four displacement waves. Thus the nanocrystalline structure formed of particles each with only one displacement wave is stabilized. One can suppose that anomalies of resistivity are caused by scattering of conduction electrons by all 4 orientations of ω clusters with dimensions compared to the mean free path of electrons. Qualitatively this phenomenon corresponds to diffraction model [9,10] used for liquid, amorphous and quasicrystalline alloys.

5. CONCLUSION

Metastable nanocrystalline structure formed by ω clusters of 4 orientations is observed in Ti rich Ti-

V, Ti-Fe quenched alloys. Anomalously large reversible increase of peak intensities of ω reflections accompanied by decrease of their width is observed if alloys with $C_{\omega} = 4.19-4.24$ are cooled to -195 °C. These changes imply increase of ω particle size alongside with approximately constant volume fraction of the ω phase. Low temperature annealing leads to stabilization of structure. Temperature dependences of resistivity correlate with these variations. Negative TCR is observed in alloys with large reversible increase of the peak intensities of ω reflections (and also mean particle size calculated from their width) on cooling and absolute value of TCR in this case is reduced after low temperature annealing. The results support the supposition that formation of nanocrystalline structure on the base of the ω clusters of different orientations is connected to interaction of conduction electrons with lattice distortions.

ACKNOWLEDGEMENTS

The work is supported by Russian foundation for basic research, grant No 05-02-17539 and 06-02-17535.

REFERENCES

- [1] K.K. McCabe and S.L. Sass // *Phil.Mag.* **23** (1971) 957.
- [2] W. Sinkler and D.E.Luzzi // *Acta metal. mater.* **42** (1994) 1249.
- [3] M. Isino // *J.Phys.Soc.Japan* **54** (1985) 3848.
- [4] A.S. Shcherbakov, A.F. Prekul and R.V. Pomoreev // *Phil.Mag. B* **47** (1983) 63.
- [5] N.B.Dyakonova and I.V.Lyasotsky // *Fizika metal.* **52** (1981)119.
- [6] I.V.Lyasotsky and N.B.Dyakonova // *Fizika metal.* **53** (1982) 1161.
- [7] B.Horovitz, J.L.Murray and J.A.Krumhansl // *Phys.Rev. B* **18** (1978) 3549.
- [8] D.T. Keating and S.J. LaPlaca // *J.Phys.Chem.Solids* **35** (1974) 879.
- [9] S.R. Nagel // *Phys.Rev. B* **16** (1977) 1694.
- [10] S.J. Poon // *Adv.Phys.* **41** (1992) 303.